NJC

RSC Publishing

PAPER

View Article Online
View Journal | View Issue

Cite this: *New J. Chem.*, 2013, **37**, 2564

Nucleation of copper on mild steel in copper chloride ($CuCl_2 \cdot 2H_2O$)–1-ethyl-3-methylimidazolium chloride [EMIM]Cl–ethylene glycol (EG) ionic liquid†

Gengan Saravanan*[ab] and Subramanian Mohan[a]

Received (in Montpellier, France) 6th March 2013,
Accepted 3rd June 2013

DOI: 10.1039/c3nj00245d

www.rsc.org/njc

A dense and adhesive Cu layer was successfully electrodeposited on mild steel in a copper chloride ($CuCl_2 \cdot 2H_2O$)–1-ethyl-3-methylimidazolium chloride [EMIM]Cl–ethylene glycol [EG] ionic liquid. The mechanism of copper nucleation is studied using cyclic voltammetry and chronoamperometry. It is observed that 3D-instantaneous nucleation leads to a bright nano-structured deposit. The morphology of the deposit was characterized SEM and X-ray diffraction techniques. The deposition method was found to take place in an environmentally friendly green electrolyte without co-ligands such as cyanide and volatile toxic solvents.

Introduction

The convergence of two distinct fields of ionic liquid chemistry, those of imidazolium salts and liquid crystals, could lead to a vast range of new materials.[1–4] Ionic liquids are composed of organic cations such as substituted pyridinium, imidazolium ions or tetraalkylammonium ions, and of organic or inorganic anions, such as $AlCl_4^-$, BF_4^-, $CF_3SO_3^-$, PF_6^- and $(CF_3SO_2)_2N^-$. Uniting the properties of imidazolium derivatives, which have low melting points, low volatility, inflammability, high chemical stability, tunable conductivity, and wide electrochemical windows, with those of liquid crystals, which have many forms of labile microscopic ordering, raises fascinating prospects.[5,6] Electrodeposition of copper is essential for a variety of industrial and decorative purposes, including large-scale use in the electronic industry for the production of printed circuit boards, and electrotypes in the printing industry. For copper plating, cyanide based electrolytes are most widely employed and are highly corrosive and suffer from several drawbacks including, toxicity, high energy consumption, and air pollution. Ionic liquids have been used as alternative green electrolytes, since they are a less environmentally hazardous option. Copper has been electrodeposited using chloroaluminate ionic liquids, some of which still remain popular.[7–10]

Endres and co-workers have shown that copper can be deposited from butylmethyl pyrrolidinium [BMP][Tf_2N] at various temperatures. This ionic liquid has limited solubility and because of this copper cations had to be introduced into the liquid *via* anodic dissolution of a copper electrode.[11] Abbott and co-workers reported copper deposition based on a choline chloride and ethylene glycol based eutectic solvent.[12] Since this eutectic solvent has a very low electrochemical window, imidazolium based ionic liquids have been used for our study because they have wider electrochemical windows.

In the current work we have seen that ionic liquids based on [EMIM]Cl and hydrogen bond donors, such as ethylene glycol, can be used as a green solvent for the electrodeposition of copper. We have used a combination of cyclic voltammetry, chronoamperometry, X-ray diffraction and scanning electron microscopy to characterize these systems.

Experimental details

In our experiment, ionic liquid whose molar ratio of $CuCl_2 \cdot 2H_2O$–[EMIM]Cl–ethylene glycol (EG) was 1 : 1 : 2 was prepared by the slow addition of a certain weight of $CuCl_2 \cdot 2H_2O$ (99.89%, Merck) to a mixture of [EMIM]Cl (99%, Merck) and EG (98%, Acros Organics) at room temperature. The mixture was continuously stirred by a magnetic bar for 2 h to ensure uniformity. All electrochemical measurements and electrodeposition experiments were carried out open to air. Electrochemical investigations, including cyclic voltammetry and potential step chronoamperometry, were carried out using a Princeton Applied Research Model PARSTAT 2273 potentiostat-galvanostat controlled by Power Suite software.

A conventional three-electrode electrochemical cell was used for these experiments. The working electrode was a platinum

[a] *(CSIR)-Central electrochemical research institute, Karaikudi-630006, India. E-mail: saravanan3che@gmail.com; Fax: +91-4565-227713; Tel: +91-4565-227551*
[b] *Yonsei University, Seoul-120749, Korea*

† Electronic supplementary information (ESI) available. See DOI: 10.1039/c3nj00245d

wire with a surface area 0.15 cm^2. The counter electrode was a platinum sheet and the reference electrode was a saturated calomel electrode (SCE) with a Luggin capillary. All potentials in the text were referred to the SCE. All voltammograms were performed at ambient temperature (28 ± 2 °C) and at various scan rates from 25 to 100 mV s^{-1}. Chronometric deposition experiments were carried out under diffusion control at an applied potential −0.70 V. A saturated calomel electrode, which has been shown to have a stable reference potential in chloride based ionic liquids,[12] was used in all electrochemical experiments. The potential window of the [EMIM]Cl–EG based ionic liquid was higher (3V) than that of ChCl–EG based eutectic solvent (2V).

The surface morphologies of the electrodeposits were characterized by scanning electron microscopy (SEM) employing a Hitachi 3000H. The crystallite size was assessed by an X-ray diffraction technique. XRD using a Phillips diffractometer with Cu-Kα (2.2 kW max) as the source. The crystallite size was calculated using the Debye–Scherrer formula.

Results and discussion

Voltammetric studies

Cyclic voltammetry (CV) data were recorded at a Pt electrode immersed in a 0.3 M $CuCl_2{\cdot}2H_2O$: 0.3 M [EMIM]Cl : 0.6 M EG ionic liquid as a function of the sweep rate, and are shown in Fig. 1A. Reduction of the Cu^{2+} ion occurred at about −0.186 V, and oxidation of Cu^{1+} occurred at about +1.074 V. Both the cathodic and the anodic peaks exhibited a linear dependence on the square root of the scan rate, as shown in Fig. 1B. The reduction of Cu^{1+} to Cu(0) occurred at −0.942 V, and the oxidation of copper was observed at +0.660 V. At lower scan rates the current corresponding to this anodic peak was much lower, since there was rapid crystallization of copper at the Pt electrode.[13] The values of the diffusion coefficients of Cu(II) and Cu(I) were found to be 8.86×10^{-7} and 1.06×10^{-6} cm^2 s^{-1}, respectively.

[EMIM]Cl as solvent and grain-refiner

For copper electrodeposition from acid sulphate solutions, Mattsson and Bockris[14] (1960) proposed a classical two-step mechanism;

$$Cu^{2+} + e^- \rightarrow Cu^+ \quad (1)$$

$$Cu^+ + e^- \leftrightarrow Cu \quad (2)$$

It was proposed that the first step in this process occurred slowly and was rate controlling with Cu^+ existing in equilibrium with Cu at the cathode surface. In the structure of the imidazolium base [EMIM]Cl, the atoms of the imidazolium ring and the –C=N– group can form a large π bond. Then, not only can the π electrons of the imidazolium base enter the unoccupied orbitals of copper to form feed back bonds. This produces more than one center of adsorption action.[15] Meanwhile, the presence of the electron donating group on the imidazolium base structure increases the electron density on the nitrogen of the –C=N– group, resulting high absorbability.[16] Therefore, [EMIM]Cl can adsorb on the cathodic surface effectively.

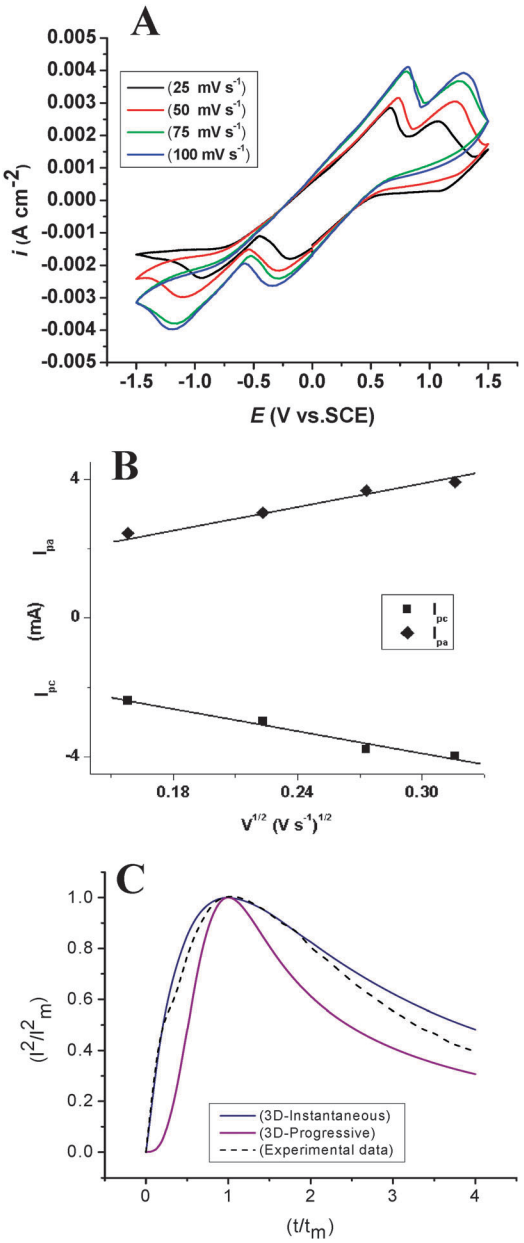

Fig. 1 (A) Cyclic voltammograms for the Pt electrode in a 0.3 M $CuCl_2{\cdot}2H_2O$: 0.3 M [EMIM]Cl : 0.6 M EG ionic liquid. Scan rate 25–100 mV s^{-1} and T = 28 ± 2 °C. (B) Plot of cathodic and anodic peaks currents against the square root of the scan rates. (C) Comparison of dimensionless time *vs.* dimensionless current (eqn (5) and (6)) for 0.3 M $CuCl_2{\cdot}2H_2O$ in 1 [EMIM]Cl : 2 EG ionic liquid following a potential step from 0 to −700 mV *vs.* SCE.

When [EMIM]Cl was added to the electrolyte, the additive molecules can adsorb at the cathodic surface and interact with the Cu^+ ions generated from eqn (1) to form a Cu–[EMIM]Cl complex (eqn (3)) by the following equilibria:

$$Cu^+ + [EMIM]Cl \leftrightarrow Cu - [EMIM]Cl^+_{ads} \quad (3)$$

$$Cu - [EMIM]Cl^+_{ads} + e^- \rightarrow Cu + [EMIM]Cl \quad (4)$$

The effect of [EMIM]Cl on the copper electroreduction process is attributed to adsorption of the complex at the active sites,

where it may accept an electron from the cathode and discharge copper atoms which are incorporated at the active sites (eqn (4)). The [EMIM]Cl hinders the surface diffusion of partially reduced adions and leads to levelled and fine-grained cathodic deposits, which are released and can then form a complex.

Chronoamperometry for nucleation modelling

In order to study the nucleation and growth mechanism, chronoamperometry (CA) was performed in the ionic liquid. In this experiment 0.3 M Cu^{2+} ions and an applied potential of −0.7 V was selected for the nucleation studies. CA is an important diagnostic electrochemical technique because it provides the current transients. These were effectively used by Scharifker and Hills[17] to derive the model. According to the models, there are two limiting nucleation mechanisms, the 3D-instantaneous and 3D-progressive. The 3D-instantaneous corresponds to a slow growth of nuclei on a small number of active sites; all activated at the same time. While the 3D-progressive nucleation corresponds to fast growth of nuclei on many active sites, all activated during the course of electro-reduction.[18]

The models for 3D-instantaneous and 3D-progressive nucleation are given by eqn (5) and (6), respectively.

$$I^2/I^2_m = 1.9542/(t/t_m)\{1 - \exp[-1.2564(t/t_m)]\}^2 \quad (5)$$

$$I^2/I^2_m = 1.2254/(t/t_m)\{1 - \exp[-2.3367(t/t_m)^2]\}^2 \quad (6)$$

Where, I_m and t_m are the current and time coordinates of the peak, respectively. Fig. 1C shows the non-dimensional plots of the 3D-instantaneous and 3D-progressive mechanisms along with the experimental data, which are represented by solid and dashed lines, respectively. The corresponding fit of the experimental data is according to the Scharifker–Hills model. The 3D-instantaneous mechanism was obtained for both current-time rising and the maximum part of the CA data. The observation presented here provides the first convincing experimental evidence in support of bright metallic coatings resulting from nano-scale deposits, which is due to 3D-instantaneous nucleation and growth mechanism.

Potentiostatic electrodeposition

The SEM micrographs in Fig. 2A and B show the surface morphology of the electrodeposited copper layer on mild steel obtained at a constant potential in 1 M $CuCl_2{\cdot}2H_2O$: 1 M [EMIM]Cl : 2 M EG ionic liquid. The particles formed by electrodeposition from the ionic liquid are distorted nano-icosahedral (250 nm) and are aggregated into multi-icosahedral.

Fig. 2C shows the X-ray diffraction pattern of the Cu films obtained for the potentiostatic deposited conditions. The film exhibits the presence of pure Cu with a FCC-icosahedra.[19] The Bragg reflections corresponding to the crystalline copper were observed at 2θ = 43.50, 50.64, 74.28 and 90.11°, which correspond to indexed planes of copper crystals: (111), (200), (220) and (311), respectively, with unit cell parameters of a = 3.615 Å (JCPDS card no.: 00-89-2838). From the width of the diffraction

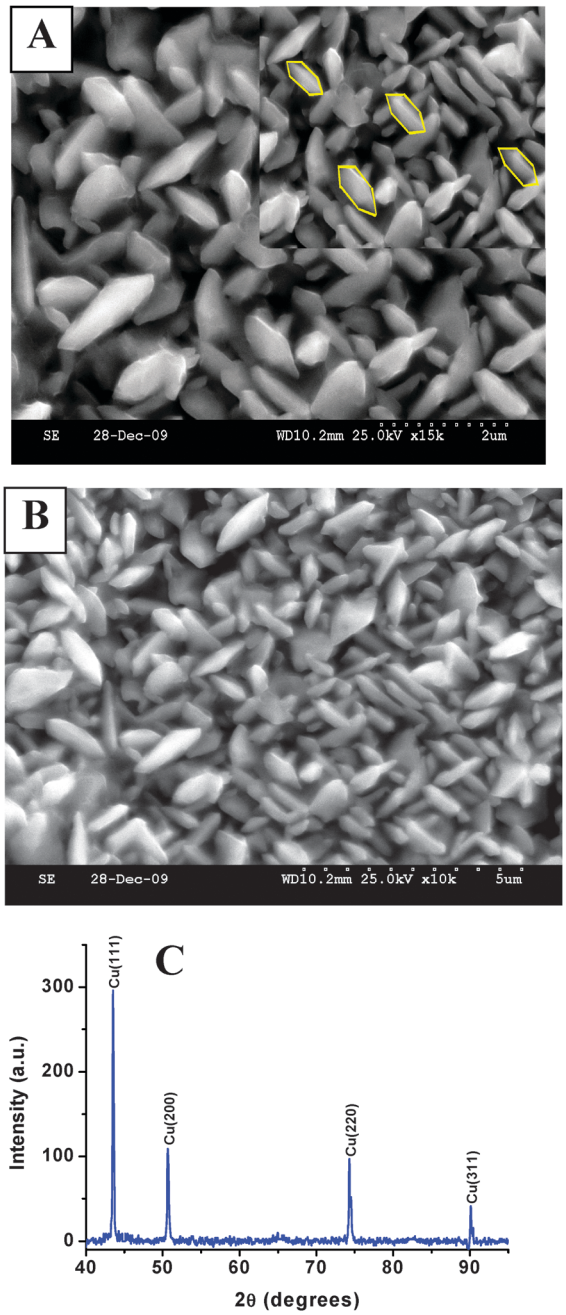

Fig. 2 (A) SEM micrographs of the electrodeposited Cu on mild steel from 1 M $CuCl_2{\cdot}2H_2O$: 1 M [EMIM]Cl : 2 M EG at −700 mV cm^{-2}, $T = 28 \pm 2$ °C, the magnification of the micrograph is 15 000×. The insert SEM picture shows the icosahedral boundaries. (B) Magnification of the micrograph is 10 000×. (C) X-Ray diffraction pattern for the copper deposits in 1 M $CuCl_2{\cdot}2H_2O$: 1 M [EMIM]Cl : 2 M EG ionic liquid.

peaks, the average crystallite size was calculated according to the Debye–Scherrer equation (eqn (7)).

The crystallite size (D) was calculated from the line broadening β[20]

$$D = \frac{0.9\lambda}{\beta \cos\theta} \quad (7)$$

Where λ is the X-ray wavelength and θ is the Bragg angle. The crystallite sizes were calculated for the different phases

present in the film and the crystallite sizes were found to be in the range of 31–76 nm. Such small crystallite sizes contribute to the smooth surface morphology and also they have a beneficial effect on the improvement of the micro hardness of the coatings.[21] Also the crystallite size reduction to the nanometer range results in considerable improvement in their corrosion resistance.[22] The strain and the dislocation density are also determined from the XRD data using the eqn (8) and (9).[23]

$$\varepsilon = \frac{\beta \cos\theta}{4} \tag{8}$$

$$\delta = \frac{n}{D^2} \tag{9}$$

Where β is the FWHM of the peak, D is the crystallite size and n is a factor, which is the unity for the thin film.[24] The calculated value of the strain and the dislocation densities are (4.5×10^{-2}, 5.38×10^{-4}). Smaller values of strain and dislocation density indicate high quality deposits. The preferred growth orientation was determined using the texture coefficient TC of a (hkl) plane, which was defined by Barrett and Massalski (eqn (10))[25] as

$$TC_{hkl} = \frac{I_{hkl}/I^0_{hkl}}{(1/N)\sum I_{hkl}/I^0_{hkl}} \tag{10}$$

Where, I^0_{hkl} is the intensity of the powder pattern in the JCPDS cards, I_{hkl} is the measured intensity of XRD and N is the number of calculated peaks. Four peaks of (111), (200), (220) and (311) were used to calculate the texture coefficient. From the values the preferred orientation of TC_{111} was found to be 32.55.

Conclusions

This work shows that an ionic liquid based on [EMIM]Cl and a hydrogen bond donor, such as EG, can be used as a cyanide free electrochemical solvent for the electrodeposition of copper at room temperature. We have presented in this paper some results about the nucleation and growth mechanism of the electrodeposited copper. From the non-dimensional plot, the nucleation conforms to a 3D-instantaneous nucleation model followed by diffusion controlled growth. SEM analysis showed that the copper deposits were nano-crystalline, and growth leads to smooth and bright metallic materials. [EMIM]Cl was found to be an efficient solvent and gave levelled to fine-grained cathodic deposits.

Acknowledgements

The authors wish to express their sincere thanks to the Director, CECRI, Karaikudi-6 for his kind permission to publish these results. Gengan Saravanan thanks the CSIR for the award of a Senior Research Fellowship. The authors also thank Mr R. Ravishanker the SEM images and S. Krithika for XRD measurements.

Notes and references

1 H. Ohno, *Electrochemical Aspects of Ionic Liquids*, Wiley-Interscience, New York, 2005.
2 P. Wasserscheid and T. Welton, *Ionic Liquids in Synthesis*, Wiley-VCH, Weinheim, 2003.
3 J. Dupont, R. F. De Souza and P. A. Z. Suarez, *Chem. Rev.*, 2002, **102**, 3667.
4 J. W. Goodbye, G. W. Gray, H.-W. Spiess, V. Vill and D. Demus, *Handbook of liquid crystals*, Wiley-VCH, Weinheim, 1998.
5 F. Endres, *ChemPhysChem*, 2002, **3**, 144.
6 D. Allen, G. Baston, A. E. Bradley, T. Gorman and A. Haile, *Green Chem.*, 2002, **4**, 152.
7 R. T. Carlin, H. C. De Long, J. Fuller and P. C. Trulove, *J. Electrochem. Soc.*, 1998, **145**, 1598.
8 B. J. Tiernry, W. R. Pitner, J. A. Mitchell, C. L. Hussey and G. R. Stafford, *J. Electrochem. Soc.*, 1998, **145**, 3110.
9 C. Nanjundiah and R. A. Osteryoung, *J. Electrochem. Soc.*, 1983, **130**, 1312.
10 F. Endres and A. Schweizer, *Phys. Chem. Chem. Phys.*, 2000, **2**, 5455.
11 S. Zein El Abedin, A. Y. Saad, H. K. Farag, N. Borisenko, Q. X. Liu and F. Endres, *Electrochim. Acta*, 2007, **52**, 2746.
12 A. P. Abbott, G. Capper, K. J. McKenzie and K. S. Ryder, *J. Electroanal. Chem.*, 2007, **599**, 288.
13 S. Marczak, P. K. Wrona and Z. Galus, *J. Electroanal. Chem.*, 1997, **436**, 79.
14 E. Mattson and J. O. M. Bockris, *Trans. Faraday Soc.*, 1959, **55**, 1586.
15 D. Q. Zhang, L. X. Gao and G. D. Zhou, *Corros. Sci.*, 2004, **46**, 3031.
16 J. Fang and J. Li, *J. Mol. Struct.*, 2002, **593**, 179.
17 B. Scharifker and G. Hills, *Electrochim. Acta*, 1983, **28**, 879.
18 M. P. Pardave, M. T. Ramirez, I. Gonzales, A. Serruya and B. R. Scharifker, *J. Electrochem. Soc.*, 1996, **143**, 1551.
19 M. Ceolin, N. Galvez and J. M. Dominguez-Vera, *Phys. Chem. Chem. Phys.*, 2008, **10**, 4327.
20 A. P. Abbott, D. Boothby, G. Capper, D. L. Davies and R. K. Rasheed, *J. Am. Chem. Soc.*, 2004, **126**, 9142.
21 A. P. Abbott, G. Capper, D. L. Davies, R. K. Rasheed and V. Tambyrajah, *Chem. Commun.*, 2003, 70.
22 C. A. Huang, C. Y. Chen, C. C. Hsu and C. S. Lin, *Scr. Mater.*, 2007, **57**, 61.
23 A. Patil, V. Patil, F.-W. Choi, H.-J. Kim, B.-H. Cho and S.-J. Yoon, *J. Electroceram.*, 2009, **23**, 214.
24 M. Koch and U. Ebarbach, *Surf. Engg.*, 1997, **13**, 157.
25 C. S. Barrett and T. B. Massalski, *Structure of Metals Crystallographic Methods*, Principles and Data, New York, Pergsmon, 1980.